$$\frac{dQ^t}{dt} = 4\pi r_s^2 D \frac{d[dT^-]_G}{dr} \quad (24)$$

where Q^t is an amount of dT^- ions stored in the Stern layer, and $[dT^-]_G$, the concentration in the Gouy–Chapman layer, is assumed to vary linearly from $[dT^-]_W$ to $[dT^-]^*$, the concentration adjacent to and hence equilibrium with the Stern layer. The distribution coefficient, k, which is independent of concentration, is defined by $[dT^-]_S^e = k[dT^-]_W$. Using eq 7, $[dT^-]_S^e = kP_{dT}[dT^-]_G$, which also resembles Henry's equation.[15] Thus, the assumption will, of course, be applied exactly only to the solution infinitely dilute in dT^-.

Now, equilibrium at the surface of the adsorbing Stern layer is assumed for all times of contact, so that $[dT^-]^* = k^{-1}[dT^-]_S^t$; hence

$$\frac{d[dT^-]_G}{dr} = \frac{[dT^-]_W - k^{-1}[dT^-]_S^t}{d_r} = \frac{[dT^-]_S^e - [dT^-]_S^t}{kd_r}$$

which by use of eq 22 becomes

$$\frac{d[dT^-]_G}{dt} = \frac{3N}{4\pi(r_s^3 - r_c^3)kd_rA}(\theta_{dT}^e - \theta_{dT}^t)$$

Hence, eq 24 is written as

$$\frac{dQ^t}{dt} = \frac{3r_s^2DN}{(r_s^3 - r_c^3)kd_rA}(\theta_{dT}^e - \theta_{dT}^t)$$

Since $dQ^t/dt = ((N/A)d\theta_{dT}^t)/dt$ from eq 21,

$$\frac{d\theta_{dT}^t}{dt} = \frac{3r_s^2D}{(r_s^3 - r_c^3)kd_r}(\theta_{dT}^e - \theta_{dT}^t)$$

which upon integration for the condition that $\theta_{dT}^t = 0$ when $t = 0$, becomes

$$\theta_{dT}^e = \theta_{dT}^e[1 - e^{-[3r_s^2D/[(r_s^3-r_c^3)kd_r]]t}] \quad (25)$$

Now, by substitution of k with $[dT^-]_S^e/[dT^-]_W$ and expression of the $[dT^-]_S^e$ by eq 23, eq 25 is written as

$$\theta_{dT}^t = \theta_{dT}^e[1 - e^{-[4\pi r_s^2AaP_{dT}D/d_rN](K_m'+[dT^-]_o)t}] \quad (26)$$

which is equivalent to eq 9.

Registry No. dTH, 50-89-5; Me-dT, 958-74-7; $(n\text{-}C_4H_9)S^+(CH_3)_2I^-$, 37127-44-9; $(n\text{-}C_{12}H_{25})S^+(CH_3)_2I^-$, 18412-81-2; $(n\text{-}C_{18}H_{37})S^+(CH_3)_2I^-$, 84040-81-3.

Photocycloaddition of 9,10-Dichloroanthracene to 1,3-Cyclohexadiene[1]

William K. Smothers, Marjorie C. Meyer, and Jack Saltiel*

Contribution from the Department of Chemistry, Florida State University, Tallahassee, Florida 32306. *Received May 3, 1982*

Abstract: Irradiation of 9,10-dichloroanthracene (DCA) in the presence of 1,3-cyclohexadiene (CHD) gives three major adducts corresponding to [2 + 2] addition of CHD to the 1,2-positions of DCA and to [4 + 4] additions of CHD to the 9,10- and 1,4-positions of DCA. The previously undetected [2 + 2] adduct is the major primary photoproduct in toluene, benzene, acetonitrile, or pyridine, provided that it is protected from shorter wavelength exciting light. The dependence of emission and product quantum yields on [CHD] demonstrates that interaction between the first excited singlet state of DCA with CHD is the first step in these reactions. The product distributions are not entirely consistent with a recently proposed algorithm for prediction of reactivity in allowed [2 + 2] and [4 + 4] photocycloadditions. DCA·CHD exciplex emission was not detected, but involvement of a singlet exciplex in the cycloadditions is strongly suggested by (a) the inverse temperature dependence of Stern–Volmer plot slopes for CHD quenching of DCA fluorescence and (b) the marked decrease of adduct quantum yields in the presence of pyridine, a known exciplex-specific quencher.

Interaction of electronically excited arenes, notably anthracenes, with 1,3-dienes has been shown to lead to [4 + 4], [4 + 2], and [2 + 2] cycloadducts.[2-10] The preferred cycloaddition mode is very sensitive to substituents on either reactant. For example, anthracene gives only [4 + 4] adduct with 2,5-dimethyl-2,4-hexadiene,[2,4] both [4 + 4] and [4 + 2] adduct with 1,3-butadiene,[8] and only [4 + 2] adduct with dimethyl muconate.[7] The mode and location of the addition are influenced by substituents at the 9,10-positions of anthracene. Thus, chlorine and bromine substitutions lead to enhanced reactivity of the terminal anthracene rings.[2,9] The striking substituent dependence on the mode of addition is illustrated by 2,5-dimethyl-2,4-hexadiene, which, as stated above, gives mainly [4 + 4] addition with anthracene, [4 + 4] and [4 + 2] addition with 9-fluoroanthracene, and only [4 + 2] addition with 9,10-dichloro- or 9,10-dicyanoanthracene.[2,4]

The formation of arene/diene singlet exciplexes was suggested to account for the quenching of arene fluorescence by 1,3-dienes[11] and later confirmed in specific cases by the observation of exciplex

(1) (a) Supported by National Science Foundation Grants No. CHE77-23852 and CHE80-26701. (b) Presented in part at the meeting of the Florida Section of the American Chemical Society, May 1979, Fort Lauderdale, FL; Abstract No. 42. (c) Taken from the Ph.D. Dissertation of W. K. Smothers, Florida State University, 1981.

(2) Yang, N. C.; Libman, J. *J. Am. Chem. Soc.* **1972**, *94*, 1405. Yang, N. C.; Libman, J.; Barrett, L., Jr.; Hui, M. H.; Loeschen, R. L. *Ibid.* **1972**, *94*, 1406.

(3) Yang, N. C.; Neywick, C.; Srinivasachar, K. *Tetrahedron Lett.* **1975**, 4313.

(4) (a) Yang, N. C.; Srinivasachar, K.; Kim, B.; Libman, J. *J. Am. Chem. Soc.* **1975**, *97*, 5006. (b) See Note Added in Proof.

(5) Yang, N. C.; Yates, R. L.; Masnovi, J.; Shold, D. M.; Chiang, W. *Pure Appl. Chem.* **1979**, *51*, 173.

(6) Kaupp, G. *Angew. Chem., Int. Ed. Engl.* **1972**, *11*, 718. Also see, Kaupp, G. *Ibid.* **1972**, *11*, 313.

(7) Kaupp, G.; Dyllick-Brenzinger, R.; Zimmerman, I. *Angew. Chem., Int. Ed. Engl.*, **1975**, *14*, 491.

(8) Kaupp, G. *Liebigs Ann. Chem.* **1977**, 254.

(9) Kaupp, G.; Gruter, H.-W. *Angew. Chem., Int. Ed. Engl.* **1979**, *18*, 881.

(10) Saltiel, J.; Townsend, D. E.; Metts, L. L.; Wrighton, M.; Mueller, W.; Rosanske, R. C. *J. Chem. Soc., Chem. Commun.* **1978**, 588.

(11) (a) Stephenson, L. M.; Whitten, D. G.; Vesley, G. F.; Hammond, G. S. *J. Am. Chem. Soc.* **1966**, *88*, 3665, 3893. (b) Stephenson, L. M.; Hammond, G. S. *Pure Appl. Chem.* **1968**, *16*, 125. (c) Stephenson, L. M.; Hammond, G. S. *Angew. Chem., Int. Ed. Engl.* **1969**, *8*, 261. (d) Evans, T. R. *J. Am. Chem. Soc.* **1971**, *93*, 2081. (e) Labianca, D. A.; Taylor, G. N.; Hammond, G. S. *Ibid.* **1972**, *94*, 3679. (f) Taylor, G. N.; Hammond, G. S. *Ibid.* **1972**, *94*, 3684, 3687.

0002-7863/83/1505-0545$01.50/0

Scheme I

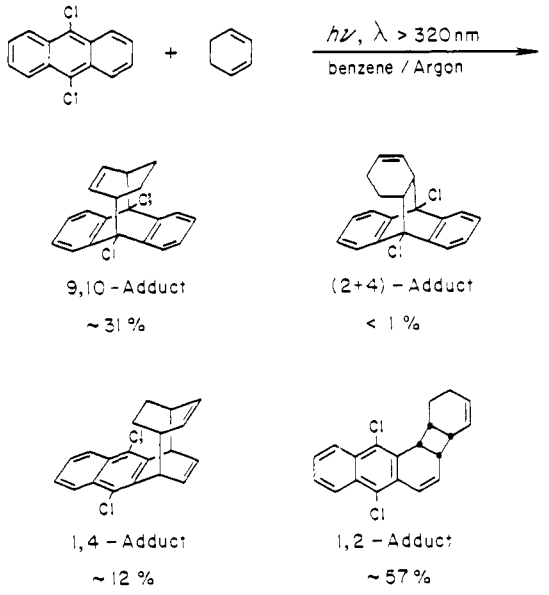

fluorescence.[5,12] The singlet exiplexes have been postulated to collapse to cycloadducts,[4,5,12d] but compelling evidence for such a mechanism has been obtained only for phenanthrene olefin systems where identical quenching efficiencies for exciplex fluorescence and cycloadduct formation are observed by using exciplex specific quenchers.[12d,13,14]

The Woodward–Hoffmann rules[15] and other molecular orbital approaches[16] predict that concerted suprafacial [4 + 2] cycloadditions are photochemically forbidden, whereas concerted suprafacial [4 + 4] or [2 + 2] photocycloadditions are allowed. For anthracene/diene systems, Yang has proposed[4,5] that formation of allowed and forbidden cycloaddition products reflects competing concerted and stepwise collapse of singlet exciplexes, with the more polar exciplexes favoring stepwise collapse leading to [4 + 2] addition. Kaupp,[6-9] on the other hand, has advanced the notion that all additions of singlet anthracenes to 1,3-dienes are stepwise, yielding diradical intermediates that either revert to ground-state addends or collapse to adducts. In contrast to these singlet pathways, the [4 + 2] photocycloadditions of benz[*a*]anthracene to the 1,3-pentadienes have been shown in our laboratory to occur exclusively from the triplet manifold,[10] indicating that arene triplets or arene/diene triplet exciplexes can also be precursors of the forbidden [4 + 2] adducts. Existence of such a triplet cycloaddition pathway is consistent with the recent report that the relative yield of [4 + 2] photoadduct from the anthracene/1,3-cyclohexadiene system increases sharply in the presence of methyl iodide.[5]

Despite numerous reports of anthracene/1,3-diene photocycloadditions,[2-9,17-19] definitive evidence clearly delineating the mechanisms of adduct formation in specific systems is sparce. This paper describes a detailed examination of photocycloaddition in the DCA/CHD system. Our findings modify Yang et al.'s product distribution[4] but support their proposal of a singlet exciplex pathway.

Table I. DCA/CHD Photoadduct Distributions[a]

[CHD], M	irradiation time, min	% DCA loss[b]	% product distribution[b] 9,10-Ad	1,2-Ad	1,4-Ad
		Benzene-d_6[c]			
0.050	180	39	32 ± 5	58 ± 5	10 ± 1
0.050	300	55	34 ± 2	54 ± 3	12 ± 1
0.050	360	92	41 ± 3	44 ± 3	15 ± 1
0.050	720[d]	61	31 ± 3	58 ± 2	11.0 ± 0.2
		Benzene[e]			
0.10_5	240	32 (33)	30 ± 1	60 ± 1 (57)	10.0 ± 0.1
0.10_5	480	60	29 ± 1	59 ± 1	12.0 ± 0.1
0.10_5	780	95 (89)	30 ± 4	60 ± 1 (57)	10 ± 1
2.2_0	40	27 (27)	31 ± 3	56 ± 2	13 ± 2
2.2_0	110	69	32 ± 1	53 ± 1	15.0 ± 0.1
2.2_0	250	100	31 ± 2	57 ± 2	12 ± 1
		Acetonitrile[f]			
0.11	138	77 (72)	11 ± 2	56 ± 1 (65)	25 ± 1
		Pyridine[g]			
0.11	600	33 (31)	17 ± 2	75 ± 1 (69)	10 ± 0.1

[a] Excitation at 404 nm at 25.0 °C using procedure 2, unless otherwise noted. [b] From relative areas for ^{1}H NMR resonances (270 MHz); number in parentheses from UV analyses. [c] Initial [DCA] = 0.039 M; procedure 1; excitation λ > 320 nm. [d] At 22 °C. [e] Initial [DCA] = 2.0×10^{-3} M. [f] Initial [DCA] = 1.5×10^{-3} M; % [MCA] = 8.2 (7.6). [g] Initial [DCA] = 2.1×10^{-3} M.

Results

Photochemical Observations. A. Preparative. Preparative-scale irradiations were carried out in benzene and acetonitrile by using conditions similar to those described by Yang et al.[4] The product distribution from a typical experiment in benzene is shown in Scheme I. The reaction was interrupted when UV analysis showed complete DCA consumption. Solvent and unreacted diene were removed by distillation, the crude adduct mixture subjected to column chromatography on activated alumina, and the partially resolved fractions separately chromatographed on silica gel/10% $AgNO_3$. Only a trace of [2 + 4] adduct was obtained in benzene and none in acetonitrile, where a small amount of 9-chloroanthracene (<3%) was obtained instead. Except for the 1,4-adduct, all adducts were obtained pure and characterized by elemental analysis in addition to NMR, UV, and IR spectroscopy. The 1,4-adduct was obtained as a mixture with 1,2-adduct. Its facile thermal rearrangement to 1,2-adduct was examined by ^{1}H NMR. Upon heating above 80 °C, the 1,4-adduct is rapidly and quantitatively converted to 1,2-adduct, $\tau_{1/2} < 5$ min; in solution at room temperature, $\tau_{1/2} \simeq 48$ h, and solid 1,4-adduct/1,2-adduct mixtures, stored at −10 °C for over a year showed no detectable change in composition. To avoid alteration of product distributions due to the thermal rearrangement, we employed short irradiation times and analyzed samples immediately following irradiation (see also section B, below). The spacial proximity assigned to the two isolated double bonds of the 1,4-adduct and the syn–cis configuration assigned to the cyclobutane moiety of the 1,2-adduct were deduced by assuming that the thermal conversion corresponds to a Cope rearrangement of 1,4-adduct:[20-22]

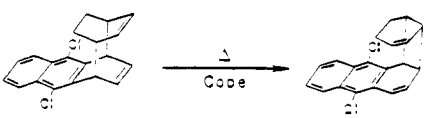

(1)

(12) (a) Taylor, G. N. *Chem. Phys. Lett.* **1971**, *10*, 355. (b) Saltiel, J.; Townsend, D. E. *J. Am. Chem. Soc.* **1973**, *95*, 6140. (c) Saltiel, J.; Townsend, D. E.; Watson, B. D.; Shannon, P. *Ibid.* **1975**, *97*, 5688. (d) Caldwell, R. A.; Creed, D. *Acc. Chem. Res.* **1980**, *13*, 45 and references therein.

(13) (a) Caldwell, R. A.; Smith, L. *J. Am. Chem. Soc.* **1974**, *96*, 2994. (b) Caldwell, R. A.; Creed, D.; DeMarco, D. C.; Melton, L. A.; Ohta, H.; Wine, P. H. *Ibid.* **1980**, *102*, 2369.

(14) (a) Majima, T.; Pac, C.; Sakurai, H. *Bull. Chem. Soc. Jpn.* **1978**, *51*, 1811. (b) Pac, C.; Sakurai, H. *Chem. Lett.* **1976**, 1067. (c) Itoh, M.; Takita, N.; Matsumoto, M. *J. Am. Chem. Soc.* **1979**, *101*, 7363.

(15) Woodward, R. B.; Hoffmann, R. "The Conservation of Orbital Symmetry"; Academic Press: New York, 1970.

(16) (a) Zimmerman, H. E. *Acc. Chem. Res.* **1971**, *4*, 272. (b) Dougherty, R. C. *J. Am. Chem. Soc.* **1971**, *93*, 7187. (c) Michl, J. *Mol. Photochem.* **1974**, *4*, 243, 257, 287.

(17) Yang, N. C.; Shold, D. M. *J. Chem. Soc., Chem. Commun.* **1978**, 978.

(18) Yang, N. C.; Masnovi, J.; Chiang, W. *J. Am. Chem. Soc.* **1979**, *101*, 6465. Also see, Caldwell, R. A. *Ibid.* **1980**, *102*, 4004.

(19) Yang, N. C.; Shou, H.; Wang, T.; Masnovi, J. *J. Am. Chem. Soc.* **1980**, *102*, 6652.

(20) Yang, N. C.; Libman, J. *J. Am. Chem. Soc.* **1972**, *94*, 9228.

(21) Grimme, W.; Mauer, W.; Reinhardt, G. *Angew. Chem., Int. Ed. Engl.* **1979**, *18*, 224.

Table II. DCA Loss and Product Yields in Acetonitrile[a]

[CHD] × 10², M	$\phi_{\text{-DCA}} \times 10^2$	$\phi_{9,10} \times 10^2$	$(\phi_{1,2} + \phi_{1,4}) \times 10^2$	$\phi_{1,2} \times 10^2$	$\phi_{\text{MCA}} \times 10^2$
			Degassed		
1.05	3.36 ± 0.16 (3.13)	0.74 ± 0.02	2.67 ± 0.11	(2.43)	[b]
1.05[c]	(3.40 ± 0.05)			(1.96 ± 0.01)	
1.47[c]	(4.23 ± 0.13)			(2.58 ± 0.03)	
2.10	6.4 ± 0.1 (6.5)	1.42 ± 0.05	4.76 ± 0.08	(4.22)	0.20 ± 0.03
2.10[c]	(5.84 ± 0.18)			(3.65 ± 0.05)	
2.10[d]	7.0 ± 0.2 (7.4)	1.41 ± 0.05	4.8 ± 0.2	(4.15)	0.70 ± 0.03
2.10[e]	7.0 ± 0.6	1.54 ± 0.05	4.6 ± 0.6		0.86 ± 0.04
3.15	(7.85 ± 0.11)		(4.87 ± 0.02)		
4.20	9.1 ± 0.4	2.36 ± 0.11	6.6 ± 0.5	(6.0 ± 0.3)	0.22 ± 0.02
	(9.42 ± 0.17)				
8.39	16.7 ± 2.2	4.0 ± 0.4	12.6 ± 1.5	(8.83 ± 0.14)	0.11 ± 0.01
	(13.6 ± 0.1)				
21.0	(18.1 ± 0.2)			(13.1 ± 1.2)	
			Air-Saturated		
1.05	2.3 ± 0.3 (2.6)	0.51 ± 0.07	1.74 ± 0.17	(1.90)	[b]
2.10	4.3 ± 0.2 (5.1)	1.05 ± 0.05	3.26 ± 0.17	(3.10)	[b]
2.10[d]	4.54 ± 0.05 (5.3)	1.01 ± 0.04	3.53 ± 0.06	(3.22)	[b]
2.10[e]	5.01 ± 0.07 (5.2)	1.14 ± 0.04	3.86 ± 0.04	(3.49)	[b]
4.20	7.9 ± 0.1 (7.8)	2.4 ± 0.3	5.5 ± 0.2	(6.0)	[b]
8.39	10.7 ± 0.9	3.2 ± 0.3	7.4 ± 0.6		[b]

[a] Irradiation at 366 nm, 25.0 °C; initial [DCA] = 4.49×10^{-4} M, unless noted otherwise; analyses by GLC, except values in parentheses are by UV; error limits are average deviations from the mean of several GLC traces and/or independent runs; see Table II-S (supplementary material) for more details. [b] MCA not detectable; $\phi_{\text{MCA}} < 7 \times 10^{-4}$. [c] Initial [DCA] = 1.15×10^{-3} M. [d] $[H_2O] = 0.55_6$ M. [e] $[H_2O]$ = 1.11 M.

A 1:1 mixture of 1,4- and 1,2-adducts was irradiated at 366 nm in cyclohexane (1.8×10^{-4} M adducts) and periodically subjected to UV and NMR analysis. This procedure was shown to selectively and quantitatively destroy the 1,2-adduct (yield DCA: 72 ± 2%) without affecting the 1,4-adduct. The UV spectrum of the 1,4-adduct, obtained by difference from these irradiated mixtures, shows no absorption at 366 nm.

B. Product Distributions. Degassed solutions of DCA and CHD were irradiated at 25.0 ± 0.1 °C with benzene-d_6, benzene, acetonitrile, and pyridine as solvents (see Experimental Section, procedures 1 and 2). Excitation was at 404 nm (filter system 2), except in one of the benzene experiments where a uranyl glass filter was employed, $\lambda > 320$ nm. Product distributions were determined by ^{1}H NMR (270 MHz), and in some instances DCA loss (~402 nm) and 1,2-adduct (~320 nm) formation were determined by UV analysis. The results are summarized in Table I. Only the 9,10-adduct, 1,2-adduct, 1,4-adduct, and, in acetonitrile, 9-chloroanthracene were detected, suggesting that the [2 + 4] adduct comprises less than 1% of the adduct mixtures. The results are consistent with those of the preparative experiments. With benzene as solvent, 404-nm excitation gives product distributions independent of CHD concentration, % conversion, or irradiation time. Identical product distributions are obtained when the exciting light is filtered through uranyl glass ($\lambda > 320$ nm), provided that conversions are kept below ~50%. At higher conversions, under these conditions, the yield of the 1,2-adduct decreases, due to competition for the incident light and photocleavage to DCA and CHD.[23] UV and NMR analysis of identical samples are in very good agreement, indicating that the 1,2-adduct is the only product with significant absorption at $\lambda = 320$ nm. In the 1,4-adduct, the naphthalene moiety is not conjugated with a double bond and its UV spectrum is shifted somewhat to the blue relative to the UV spectrum of the 1,2-adduct (see Experimental Section).

C. Photoreaction Quantum Yields. DCA loss and photoproduct quantum yields were determined as a function of [CHD] in acetonitrile (Table II), toluene, benzene, and pyridine (Table III) solution. Irradiations were conducted in a Moses merry-go-round apparatus[24] at 25.0 ± 0.1 °C with 366-nm excitation. The benzophenone-sensitized isomerization of *trans*-stilbene was used for

Table III. DCA Loss and Product Quantum Yields in Toluene, Benzene, and Pyridine[a]

[CHD], M	$\phi_{\text{-DCA}} \times 10^2$	$\phi_{9,10} \times 10^2$	$(\phi_{1,2} + \phi_{1,4}) \times 10^2$	$\phi_{1,2} \times 10^2$
		Toluene[b]		
0.105	4.4 ± 0.2	1.9 ± 0.1	2.6 ± 0.1	
0.210	7.5 ± 0.2	3.4 ± 0.1	4.1 ± 0.2	
0.420	11.0 ± 1.1	5.7 ± 0.4	5.2 ± 0.7	
0.839	16.1 ± 0.8	9.9 ± 0.5	6.2 ± 0.6	
		Benzene[c]		
0.105	5.01 ± 0.03			2.96 ± 0.09
0.126	6.08 ± 0.01			3.48 ± 0.03
0.210	9.51 ± 0.30			5.38 ± 0.04
0.420	14.6 ± 0.1			8.36 ± 0.25
0.839	20.6 ± 0.3			11.7 ± 0.1
1.68	27.2 ± 1.0			15.9 ± 0.5
2.20	30.0 ± 0.2			15.8 ± 0.1
		Pyridine[c]		
0.0420	1.14 ± 0.01			0.760 ± 0.003
0.0525	1.27 ± 0.01			0.850 ± 0.005
0.0629	1.42 ± 0.01			0.923 ± 0.003
0.0839	1.60 ± 0.01			1.12 ± 0.01
0.126	1.88 ± 0.03			1.22 ± 0.11
0.210	2.17 ± 0.02			1.52 ± 0.01
0.629	2.92 ± 0.03			2.00 ± 0.02
		Pyridine/Benzene[d]		
0.208[e]	9.03 ± 0.1[f]	4.1 ± 0.1	5.0 ± 0.2	
0.208[g]	7.52 ± 0.2	3.2 ± 0.1	4.1 ± 0.2	
0.208[h]	8.4 ± 0.3	3.8 ± 0.1	4.6 ± 0.3	
0.208[i]	9.2 ± 0.4	3.6 ± 0.2	5.6 ± 0.5	

[a] For more details, see Tables II-S and III-S (supplementary material). Excitation at 366 nm, 25.0 °C, unless noted otherwise. [b] $[DCA]_0 = 9.09 \times 10^{-4}$ M; GLC analyses, average deviation from the mean from several traces and/or independent runs. [c] $[DCA]_0$ $= 2.04 \times 10^{-3}$ and 1.03×10^{-3} M for benzene and pyridine, respectively; UV analyses, average deviation from the mean from duplicate solutions and different irradiation times. [d] 404-nm excitation; $[DCA]_0 = 1.15 \times 10^{-3}$ M. [e] Benzene solvent. [f] Intrapolated value used as actinometer. [g] Benzene solvent includes azulene, 1.67×10^{-3} M. [h] 0.993 M pyridine in benzene. [i] 1.99 M pyridine in benzene.

(22) Yang, N. C.; Libman, J.; Savitzky, M. *J. Am. Chem. Soc.* **1972**, *94*, 9226.

(23) The photochemistry and photophysics of the 1,2- and 9,10-adducts have been investigated in some detail and will be reported separately: Smothers, W. K.; Saltiel, J. *J. Am. Chem. Soc.*, in press.

Table IV. Quenching of DCA Fluorescence by Oxygen, 25.0 ± 0.5 °C

solvent	$[O_2]$,[a] M × 10^3	I_0/I_{ox}	τ_m, ns	$k_{qm} \times 10^{-10}$, M^{-1} s^{-1}
benzene[b]	1.6_7	1.30	9.78[f]	1.8_4
pyridine[b]	1.1_6	1.17	9.3[g]	1.5_8
toluene[c]	1.9_7	1.34	10.4[h]	1.6_6
acetonitrile[d]	1.8[e]	1.39	10.6[i]	2.0_9

[a] For air-saturated solution at 25.0 °C (see: Gjaldbak, J. C. *Acta Chem. Scand.* 1952, *6*, 623, unless otherwise noted). [b] Excitation 350 nm, emission 433 nm, [DCA] = 4.5×10^{-5} M. [c] As in *b* except excitation at 340 nm. [d] As in *b* except emission monitored at 429 nm, [DCA] = 2.3×10^{-5} M. [e] Estimated assuming $k_q = 2.1 \times 10^{10}$ M^{-1} s^{-1} and using the known DCA fluorescence lifetime in degassed solution. [f] Average of values in ref 12c and 29. [g] Estimated, see text. [h] Reference 29a. [i] Reference 12c.

actinometry.[25,26] Conversions to *cis*-stilbene, corrected for zero-time cis content and back reaction[27] ranged from 1.00 to 6.00%. As many as three actinometers were irradiated in series with the same DCA/CHD samples and/or the initial [*trans*-stilbene] was adjusted, 1.57 to 11.7×10^{-2} M, to avoid larger conversions. The benzophenone concentration was 0.050 M, except for samples with the higher *trans*-stilbene concentrations in which it was 0.074 M. Results from duplicate actinometer solutions were in excellent agreement. DCA loss and photoproduct yields were measured by GLC and/or UV: GLC analysis detects DCA, MCA, 9,10-adduct, and 1,2-adduct, but the 1,4-adduct rearranges in the injection port (~145 °C) and analyzes as 1,2-adduct; UV analysis gives DCA loss (~402 nm) and 1,2-adduct appearance (~320 nm). Most DCA losses were between 11 and 21% and never exceeded 27%. One set of measurements was carried out with benzene/pyridine solvent mixtures by using 404-nm light.[28] Included in this set was a benzene solution containing 1.67×10^{-3} M azulene.

Spectroscopic Measurements. Quenching of DCA fluorescence by CHD was determined in benzene, pyridine, toluene, and acetonitrile degassed solutions by measuring relative emission intensities at the λ_{max} of the $1 \leftarrow 0$ band (~430 nm) of the DCA spectrum as a function of [CHD], Tables IV-S and V-S (supplementary material). Excitation was either at 340 or 350 nm at 25.0 °C. Additional temperatures were employed for toluene and acetonitrile. Shapes of the DCA fluorescence profiles were not detectably altered by CHD; DCA/CHD exciplex emission was not detected. Quenching of DCA fluorescence by azulene was determined in air-saturated benzene at 25.0 °C, Table VI-S (supplementary material). Under the conditions of this experiment, benzene solutions containing only azulene at the concentrations employed gave negligible emission at the monitoring wavelength (<5.0%).

Fluorescence quenching measurements were also carried out in the presence of air, at 25.0 °C. Results in acetonitrile and pyridine can be found in Table VII-S (supplementary material). Corresponding observations in benzene and toluene are not reported because it was found that freshly air-purged benzene solutions containing CHD give smaller DCA fluorescence intensities, I_{ox}, than after storage in a stoppered cuvette in the dark for several minutes. The decrease in I_0/I_{ox} with time is most pronounced at the highest diene concentrations and becomes even more striking when oxygen-purged solutions are monitored. I_0/I_{ox} ratios eventually stabilize at a value close to the corresponding degassed I_0/I ratio, and repurging of stored solution with air/oxygen gives back the initially obtained I_0/I_{ox} ratio. I_0/I_{ox} values remain constant with time in the presence of CHD with pyridine or acetonitrile as solvents,[28b] and in the absence of CHD in all four solvents (Table IV). Also shown in Table IV are oxygen concentrations in air-saturated solutions, literature values of DCA fluorescence lifetimes (τ_m) in degassedsolutions, and calculated rate constants for the quenching of ^{1}DCA* fluorescence by oxygen, k_{qm}. No changes with dark storage time could be detected in degassed solution I_0/I ratios.

Scheme II

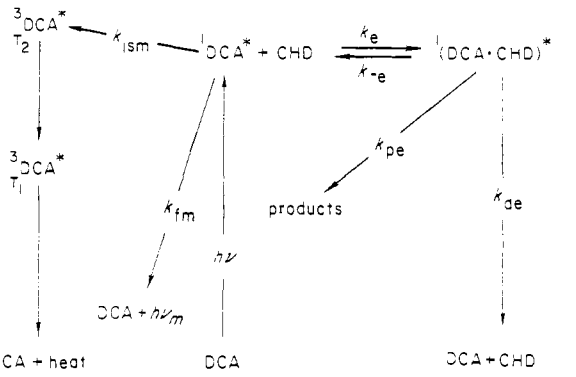

Discussion

The results in Table I show that the relative yields of 9,10-adduct, 1,2-adduct, and 1,4-adduct are independent of [CHD] and DCA conversion when 404-nm excitation is employed. An apparent trend to higher 9,10-adduct yields as [CHD] is increased in toluene (Table III) was not borne out in experiments in other solvents (Tables I–III) and was traced to analyses problems when aged GLC columns are employed. The product distribution is also not very sensitive to solvent changes when one considers the wide variation of polarity in the solvents used. 1,2-Adduct is the major primary photoproduct in all solvents. Its thermal formation from 1,4-adduct is much too slow to alter significantly product distributions in the short elapsing time between the start of the irradiations and the completion of the product analyses. The earlier failure to detect 1,2-adduct in benzene[4] was probably due to overirradiation through the uranyl glass filter employed.[4b] Such filters do not eliminate the 334- and 366-nm Hg lines that are absorbed by the 1,2-adduct and not by the other adducts. Since the major fate of excited 1,2-adduct is splitting to DCA (~72%) and CHD, overirradiation should recycle the 1,2-adduct to the other two major adducts. The results in Table I also show that product distributions in benzene are independent not only of [CHD] but also of [DCA]. In this respect, this system differs from the anthracene/CHD system where product distributions appear to be influenced by anthracene concentration.[19] In the following, the mechanistic implications of the observed concentration effect on quantum yields will be considered.

Spectroscopic Observations. The fluorescence quenching data reported in Tables IV-S–VII-S are consistent with a mechanism involving reversible singlet exciplex formation, ^{1}(DCA·CHD)*, between excited -singlet 9,10-dichloroanthracene, ^{1}DCA*, and CHD (Scheme II). The rate constants in Scheme II are self-explanatory. Exciplex fluorescence is not included since none was observed, but k_{de} includes all exciplex decay processes except dissociation, k_{-e}, that do not give products. Application of the steady-state approximation to ^{1}DCA* and ^{1}(DCA·CHD)* gives

$$I_0/I = 1 + pk_e\tau_m[CHD] \quad (2)$$

as the Stern–Volmer expression for diene quenching of DCA fluorescence where $\tau_m = (k_{fm} + k_{ism})^{-1}$ is the ^{1}DCA* lifetime in the absence of quenchers and $p = (k_{de} + k_{pe})/(k_{-e} + k_{de} + k_{pe})$ is the fraction of exciplexes that do not regenerate ^{1}DCA*. The data adhere closely to eq 2, Figure 1 is typical, and give Stern–

(24) Moses, F. G.; Liu, R. S. H.; Monroe, B. M. *Mol. Photochem.* **1969**, *1*, 245.
(25) Hammond, H. A.; DeMeyer, D. E.; Williams, J. L. R. *J. Am. Chem. Soc.* **1969**, *91*, 5180.
(26) Valentine, D., Jr.; Hammond, G. S. *J. Am. Chem. Soc.* **1972**, *94*, 3449.
(27) Saltiel, J.; Marinari, A.; Chang, D. W.-L.; Mitchener, J. C.; Megarity, E. D. *J. Am. Chem. Soc.* **1979**, *101*, 2982.
(28) (a) For a detailed description of these experiments, see: Smothers, W. K. Ph.D. Dissertation, The Florida State University, 1981. (b) We thank D. W. Eaker for experiments leading to this conclusion.
(29) (a) Ware, W. R. *J. Phys. Chem.* **1962**, *66*, 455. (b) Ware, W. R.; Baldwin, B. A. *J. Chem. Phys.* **1964**, *40*, 1703.
(30) Ware, W. R.; Baldwin, B. A. *J. Chem. Phys.* **1965**, *43*, 1194.

Table V. Stern-Volmer Constants for CHD Quenching of DCA Fluorescence and Related Parameters

solvent	$T \pm 0.5$, °C	$pk_e\tau_m$,[a] M^{-1}	τ_m,[b] ns	$pk_e \times 10^{-8}$, M^{-1} s^{-1}	k_{dif}[c] $\times 10^{-9}$, M^{-1} s^{-1}	p[d]
CH_3CN	40.0	$8.9_7 \pm 0.1$	8.8	10.2	17.8	0.057_3
CH_3CN	25.0	13.5 ± 0.1	10.6	12.7	15.5	0.081_9
CH_3CN	10.0	20.8 ± 0.1	12.7	16.4	13.3	0.12_3
$C_6H_5CH_3$	25.0	0.89 ± 0.04	10.4	0.85_6	9.70	0.008_8
$C_6H_5CH_3$	0.0	1.27 ± 0.07	12.5	1.0_2	6.37	0.016_0
$C_6H_5CH_3$	−20.0	1.77 ± 0.09	13.8	1.2_8	4.29	0.029_8
C_6H_6	25.0	1.34 ± 0.02	9.78	1.3_7	8.77	0.015_6
C_6H_6/C_5H_5N[e]	25.0	1.64 ± 0.03	9.74[g]	1.6_8	8.53[g]	0.019_7
C_6H_6/C_5H_5N[f]	25.0	2.01 ± 0.01	9.70[g]	2.0_7	8.29[g]	0.025_0
C_5H_5N	25.0	13.30 ± 0.04	9.3	14.3	6.00	0.23_8

[a] Slopes of Stern-Volmer plots; least-squares analysis with intercepts forced through unity; ranges are standard deviations. [b] For 25.0 °C values, see Table IV; otherwise see text. [c] Reference 47, see text. [d] Lower limit, see text. [e] [PY] = 0.993 M. [f] 1.99 M. [g] Intrapolated value based on mole fractions of benzene and pyridine.

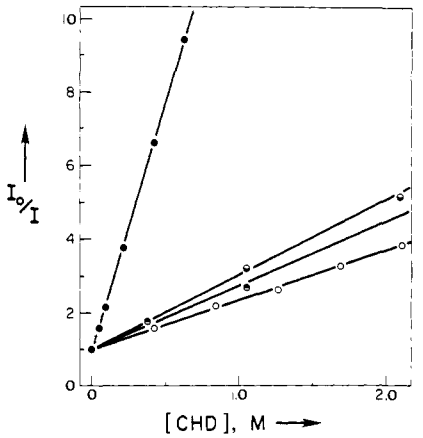

Figure 1. CHD quenching of DCA fluorescence in degassed pyridine (●), benzene, (○), 0.99 M pyridine in benzene (◓), 1.99 M pyridine in benzene (◒); 25.0 °C.

Volmer constants $pk_e\tau_m$ listed in Table V.

Conversion of the $pk_e\tau_m$ values to pk_e requires τ_m values for all conditions employed. While many of these values are available in the literature, some must be estimated by using indirect procedures. Unimolecular decay of ^{1}DCA* and other meso-substituted anthracenes consists of a temperature-independent k_{fm} and a temperature-dependent k_{ism}

$$(1/\tau_m) = k_{fm} + k^0_{ism} \exp(-E_{ism}/RT) \quad (3)$$

where k^0_{ism} and E_{ism} are Arrhenius parameters for intersystem crossing from S_1. The latter is to a higher triplet state (T_n, $n > 1$) nearly isoenergetic with S_1 and designated as T_2 in Scheme II.[31-35] Experimental determinations of the temperature dependence of ϕ_{fm} and/or τ_m of ^{1}DCA* have yielded (E_{ism}, log k^0_{ism}) values of (3.8, 10.53),[30] (4.1, 10.73),[36] (4.5, 11.23),[37] (4.4, 10.10),[30] and (3.3, 9.79),[36] where E_{ism} is in kcal/mol and k^0_{ism} is in s^{-1}, for ethanol, ethanol, heptane, hexane, and toluene as solvent, respectively.[28] With the exception of the values for hexane, these parameters follow an isokinetic relationship thus showing the expected compensation between E_{ism} and log k^0_{ism}.[38] While it is not clear to what extent this compensation reflects experimental errors, an activation energy, E_{ism}, of about 4 kcal/mol has been established, especially in the case of ethanol where two independent studies give very similar results. To obtain the solvent dependence of E_{ism}, we relied on the results of a careful study of 9,10-dibromoanthracene in which the activation energy *in* a specific solvent, E^s_{ism}, was shown to follow the empirical equation

$$E^s_{ism} = E^0_{ism} - 0.69(\nu_{01}{}^s - \nu_{01}{}^0) \quad (4)$$

where ν_{01} is the frequency in cm^{-1} of $1 \leftarrow 0$ band of the fluorescence spectrum and E^0_{ism} and $\nu_{01}{}^0$ are values for a reference solvent.[39] Using ethanol as the reference solvent and applying eq 4 to DCA gives 4.1 and 4.6 kcal/mol as the E_{ism} values for acetonitrile and toluene, respectively. The corresponding log k^0_{ism} values, 10.69 and 10.87, were chosen to conform to the experimental ϕ_{fm} and τ_{fm} values at 25.0 °C. In the case of pyridine, τ_m was calculated by using Berlman's oxygen quenching method[40] and the observations in Table IV.[41] The results in Table IV are consistent with those previously reported for DCA. They are noteworthy because they reflect smaller oxygen quenching rate constants, k_{qm}, for ^{1}DCA* than for anthracene and other aromatic hydrocarbons,[29a,41-43] indicating either that the process is not fully diffusion controlled in this case,[12c,29a] or that the presence of the chlorine atoms significantly diminishes the rate constant for DCA diffusion. k_{qm} was assumed to be a linear function of η^{-1} [44] to obtain τ_m in pyridine. Calculated and, when available, experimental τ_{fm} values are given in Table V, along with pk_e values derived from the Stern-Volmer constants.

Unique definition of the values of p requires transient fluorescence quenching measurements in addition to the steady-state observations described above.[45] In the absence of these transient measurements, lower limits for p can be obtained by assigning all quenching inefficiency to exciplex disociation, $k_e = k_{dif}$. In the case of DCA/2,5-dimethyl-2,4-hexadiene, the measured values of $k_e = 1.0 \times 10^{10}$ and 3.2×10^9 M^{-1} s^{-1} for acetonitrile and benzene, respectively, are within a factor of 2 to 3 of k_{dif}.[12c] Other experimental k_e values in arene/olefin systems with emissive exciplexes are likewise close to k_{dif}.[46] Diffusion rate constants for toluene and acetonitrile, obtained from Arrhenius parameters for fully diffusion-controlled triplet energy transfer, are shown in Table V.[47] The k_{dif} values for benzene and pyridine were based on those for toluene by adjusting for the differences

(31) Bennett, R. G.; McCartin, P. J. *J. Chem. Phys.* **1966**, *44*, 1969.
(32) Lim, E. C.; Laposa, J. D.; Yu, J. M. H. *J. Mol. Spectrosc.* **1966**, *19*, 412.
(33) Hunter, T. F.; Wyatt, R. F. *Chem. Phys. Lett.* **1970**, *6*, 221.
(34) Widman, R. P.; Huber, J. R. *J. Phys. Chem.* **1972**, *76*, 1524.
(35) Gillispe, G. D.; Lim, E. C. *Chem. Phys. Lett.* **1979**, *63*, 355.
(36) Bowen, E. J.; Sahu, J. *J. Phys. Chem.* **1959**, *63*, 4.
(37) Dreeskamp, H.; Pabst, J. *Chem. Phys. Lett.* **1979**, *61*, 262.
(38) Saltiel, J.; D'Agostino, J. T. *J. Am. Chem. Soc.* **1972**, *94*, 6445 and references cited therein.
(39) Wu, K.-C.; Ware, W. R. *J. Am. Chem. Soc.* **1979**, *101*, 5906.
(40) Berlman, I. B. "Handbook of Fluorescence Spectra of Aromatic Molecules", 2nd ed.; Academic Press: New York, 1971.
(41) (a) Stevens, B.; Algar, B. E. *J. Phys. Chem.* **1968**, *72*, 2582. (b) Stevens, B.; Dubois, J. T. *Trans. Faraday Soc.* **1963**, *59*, 2813.
(42) Parmenter, C. S.; Rau, J. D. *J. Chem. Phys.* **1969**, *51*, 2242.
(43) (a) Patterson, L. K.; Porter, G.; Topp, M. R. *Chem. Phys. Lett.* **1970**, *7*, 612. (b) Gijzeman, O. L. J.; Kaufman, K.; Porter, G. *J. Chem. Soc., Faraday Trans. 2*, **1973**, *69*, 708.
(44) Least-square analysis of the literature data cited and present results give $k_{qm} = 1.26 \times 10^{10} + (2.85 \times 10^7)\eta^{-1}$, where η is in poise.[28]
(45) Lewis, C.; Ware, W. R. *Mol. Photochem.* **1973**, *5*, 261.
(46) (a) Ware, W. R.; Watt, D.; Holmes, J. D. *J. Am. Chem. Soc.* **1974**, *96*, 7853. (b) Ware, W. R.; Holmes, J. D.; Arnold, D. R. *Ibid.* **1974**, *96*, 7861.
(47) Saltiel, J.; Shannon, P. T.; Zafiriou, O. C.; Uriarte, A. K. *J. Am. Chem. Soc.* **1980**, *102*, 6799.

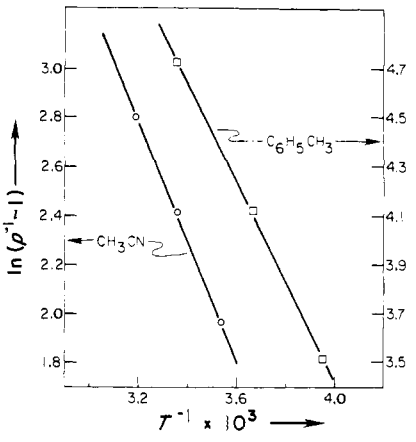

Figure 2. Plot of data according to eq 6: acetonitrile (○), toluene (□).

in viscosity. Also shown in Table V are the resulting lower limits for p, which, with previous measurements as guide, should not deviate from the exact values by more than a factor of 4.

Since no exciplex emission could be detected in the DCA/CHD system, the need for such an intermediate might well be questioned. It should be realized, however, that regardless of the nature of the fluorescence quenching process, the p values listed in Table V serve as a direct measure of the fraction of encounters between ^{1}DCA* and diene that result in disappearance of excited monomer. Examination of these p values reveals that the quenching efficiency per encounter at 25 °C is substantially less than unity in all solvents investigated. Thus if Scheme II and $k_e = k_{dif}$ are correct assumptions, then ^{1}(DCA·CHD)* dissociation to ^{1}DCA* is a significant process and the magnitude of p should be sensitive to parameters that influence exciplex decay.

The inverse temperature dependence of the $pk_e\tau_m$ values in acetonitrile and toluene (Table V) is characteristic of reversibly formed exciplexes and excimers.[48] The increase in Stern–Volmer constants with decreasing temperature reflects complementary increases in τ_m and pk_e. The inverse temperature dependence in pk_e provides strong evidence indicating that fluorescence quenching in this system is a consequence of reversible exciplex formation. The limiting p values in Table V allow estimation of differences in activation enthalpies and entropies between the process of exciplex dissociation k_{-e} and overall exciplex decay, $(k_{de} + k_{pe}) = \tau_e^{-1}$,

$$\left(\frac{1}{p} - 1\right) = k_{-e}\tau_e \tag{5}$$

$$\ln\left(\frac{1}{p} - 1\right) = \left\{\left(\Delta S^{\ddagger}_{-e} - \Delta S^{\ddagger}_{1/\tau_e}\right) - \left(\Delta H^{\ddagger}_{-e} - \Delta H^{\ddagger}_{1/\tau_e}\right)/T\right\}/R \tag{6}$$

The activation parameters for exciplex decay, $\Delta S^{\ddagger}_{1/\tau_e}$ and $\Delta H^{\ddagger}_{1/\tau_e}$, in eq 6 have qualitative significance because $1/\tau_e$ represents a sum of rate constants whose activation parameters may differ.[12d] The data adhere nicely to eq 6 (Figure 2): correlation coefficients $r^2 > 0.999$, $\Delta H^{\ddagger}_{-e} - \Delta H^{\ddagger}_{1/\tau_e}$ values of 4.90 and 4.04 kcal/mol, and $\Delta S^{\ddagger}_{-e} - \Delta S^{\ddagger}_{1/\tau_e}$ values of 21.2 and 22.9 eu in acetonitrile and toluene, respectively. These values are consistent with those reported for other olefin/arene exciplexes.[48] If activation parameters for ^{1}(DCA·CHD)* decay fall within the range of reported values for related systems, the ranges for the activation parameters for ^{1}(DCA·CHD)* dissociation obtained are $\Delta H^{\ddagger}_{-e}$ = 4–10 kcal/mol and $\Delta S^{\ddagger}_{-e}$ = 10–24 eu. The observed increase in $\Delta H^{\ddagger}_{-e} - \Delta H^{\ddagger}_{1/\tau_e}$ with increased solvent polarity is consistent with the expected increase in $\Delta H^{\ddagger}_{-e}$ due to enhanced exciplex stabilization by the polar solvent. The polar character of the exciplex is reflected in small yields of MCA in acetonitrile (Table II), which suggest an increased role for full electron transfer in this solvent (see below).[49]

Since k_{-e} can be no faster than the rate of diffusion apart from an encounter complex, i.e., $k_{-e} \leq k_{-dif} = \xi k_{dif}$ where ξ is the solvent molarity,[47] appropriate substitution of p and k_{dif} values from Table V into eq 5 gives lower limits for τ_e: $\tau_e \geq 0.03_3$, 1.2, 0.6_4, and 0.04_3 ns in acetonitrile, toluene, benzene, and pyridine, respectively.

Fluorescence quenching measurements in the presence of oxygen can also be useful in detecting the presence of reversibly formed exciplexes.[12c,50,51] Inclusion of the expected quenching processes,

$$^1\text{DCA}^* + O_2 \xrightarrow{k_{qm}} \text{DCA} + O_2 \tag{7}$$

$$^1(\text{DCA·CHD})^* + O_2 \xrightarrow{k_{qe}^{ox}} \text{DCA} + \text{CHD} + O_2 \tag{8}$$

in Scheme II gives the Stern–Volmer expression

$$I_0/I_{ox} = 1 + k_{qm}\tau_m[O_2] + p_{ox}k_e\tau_m[\text{CHD}] \tag{9}$$

where

$$p_{ox} = (1 + k_{qe}^{ox}\tau_e[O_2])/(1 + k_{-e}\tau_e + k_{qe}^{ox}\tau_e[O_2]) \tag{10}$$

Equation 9 relates the ratio of ^{1}DCA* fluorescence intensity in the absence of quenchers to the intensity, I_{ox}, in the presence of oxygen and varying concentrations of CHD. When an exciplex is formed reversibly and is sufficiently long-lived to be associated with a significant $k_{qe}^{ox}\tau_e[O_2]$ term, the slope of the Stern–Volmer plot is enhanced by the presence of oxygen (compare eq 2 and eq 9). The results obtained for air-saturated solutions of acetonitrile and pyridine (Table VII-S) give lines that are parallel to those obtained in degassed solutions, slopes 13.4 and 13.3 M^{-1}, respectively. It follows that $p = p_{ox}$ in these solvents. This result is compatible either with essentially irreversible exciplex formation, $k_{-e}\tau_e << 1$, or with reversible formation of a short-lived exciplex, $k_{qe}^{ox}\tau_e[O_2] << 1$.[12c,50] The temperature dependence of p leads to a strong preference for the second possibility, and since $k_{qe}^{ox}[O_2]$ values are usually close to $k_{qm}[O_2]$ values,[12c,50,51] limiting values of $\tau_e < 3$ and < 5 ns are calculated for acetonitrile and pyridine, respectively. This method could not be applied to fluorescence quenching observations in the presence of air in benzene and toluene because in these solvents oxygen is depleted in a dark reaction with CHD.

Information concerning the behavior of the ^{1}(DCA·CHD)* exciplex in benzene was sought with the use of pyridine as a potential exciplex quencher. The choice of pyridine was prompted by reports of quenching of photoproduct formation and/or exciplex emission by pyridine in arene/amine and arene/diene systems.[52–54] The quenching process appears to involve charge-transfer interaction between the exciplex and a pyridine molecule rather than a medium effect such as a change in solvent polarity. The possibility that the quenching may involve reversible formation of an intermediate triplex has also been suggested.[54] Advantages of pyridine over oxygen are that higher concentrations can be employed conveniently and that the quenching is specific to the exciplex. For example, the presence of 0.99 M pyridine in diene-free benzene causes no detectable change in the intensity or shape of DCA fluorescence relative to neat benzene. Moreover, the 9.3-ns ^{1}DCA* lifetime in degasses pyridine, estimated from

(48) Leading references are: (a) Stevens, B. *Adv. Photochem.* **1971**, *8*, 161. (b) Chapman, O. L.; Lura, R. D. *J. Am. Chem. Soc.* **1970**, *92*, 6352. Saltiel, J.; D'Agostino, J. T.; Chapman, O. L.; Lura, R. D. *Ibid.* **1971**, *93*, 2804. (c) Lewis, F. D.; Hoyle, C. E. *Ibid.* **1975**, *97*, 5950; **1977**, *99*, 3779. (d) Creed, D.; Wine, P. H.; Caldwell, R. A.; Melton, L. A. *Ibid.* **1976**, *98*, 621. (e) Yang, N. C.; Shold, D. M.; McVey, J. K. *Ibid.* **1975**, *97*, 5004.

(49) Smothers, W. K.; Schanze, K. S.; Saltiel, J. *J. Am. Chem. Soc.* **1979**, *101*, 1895.

(50) Charlton, J. L.; Townsend, D. E.; Watson, B. D.; Shannon, P.; Kowalewska, N.; Saltiel, J. *J. Am. Chem. Soc.* **1977**, *99*, 5992.

(51) Caldwell, R. A.; Maw, T.-S. *J. Photochem.* **1979**, *11*, 165.

(52) Soloveichik, O. M.; Ivanov, V. L.; Kuz'min, M. G. *Zh. Org. Khim., Engl. Ed.* **1976**, *12*, 860.

(53) (a) Majima, T.; Pac, C.; Sakurai, H. *Bull. Chem. Soc. Jpn.* **1978**, *51*, 1811. (b) Pac, C.; Sakurai, H. *Chem. Lett.* **1976**, 1067.

(54) Itoh, M.; Takita, N.; Matsumoto, M. *J. Am. Chem. Soc.* **1979**, *101*, 7363.

I_0/I_{ox} in the absence of CHD, is not significantly smaller than the τ_m values in the other solvents (Table IV). Incorporation of the exciplex quenching process

$$^1(\text{DCA·CHD})^* + \text{PY} \xrightarrow{k_{qe}^{py}} \text{DCA} + \text{CHD} + \text{PY} \quad (11)$$

into Scheme II leads to the Stern–Volmer expression

$$I_0/I = 1 + p_{py}k_e\tau_m[\text{CHD}] \quad (12)$$

where

$$p_{py} = (1 + k_{qe}^{py}\tau_e[\text{PY}])/(1 + k_{-e}\tau_e + k_{qe}^{py}\tau_e[\text{PY}]) \quad (13)$$

Since formation of a triplex is not required to account for the observations described herein, it is not included as a quenching process. However, the observed p/p_{ox} ratio of unity in pyridine solvent does suggest that if a ^{1}(DCA·CHD·PY)* triplex formed reversibly it is too short-lived to be quenched appreciably by oxygen in air-saturated solution.

In accord with eq 12 and 13, inclusion of pyridine in benzene increases Stern–Volmer plot slopes for DCA fluorescence quenching by CHD (Figure 1, Table V). Since CHD quenching is more efficient in neat pyridine (ϵ = 13) than in acetonitrile (ϵ = 39), assignment of the slope enhancement primarily to quenching of ^{1}(DCA·CHD)* by pyridine rather than to the small increase in bulk solvent polarity seems reasonable (benzene's dielectric constant is 2.3). Intrapolated values for τ_m and k_{dif} at the two pyridine concentrations are given in Table V, along with corresponding $p_{py}k_e$ and limiting p_{py} values. Combining eq 5 and 13 gives

$$\left(\frac{1}{p} - 1\right)\Big/\left(\frac{1}{p_{py}} - 1\right) = 1 + k_{qe}^{py}\tau_e[\text{PY}] \quad (14)$$

where p and p_{py} are limiting quenching efficiencies for CHD in benzene and in benzene/pyridine mixtures, respectively. The data when plotted according to eq 14 give $k_{qe}^{py}\tau_e = 0.31 \pm 0.02$ with least-squares-fit intercept = 0.99 ± 0.02 and $r^2 = 0.994$. The adherence to eq 14 provides further evidence suggesting that τ_e is not very sensitive to small changes in bulk solvent polarity. The range of k_{qe}^{py} values obtained from exciplex fluorescence measurements in other systems is 6.9×10^6 to 7.1×10^7 M^{-1} s^{-1}.[52-54] If the present k_{qe}^{py} value lies in this range, the calculated τ_e range for benzene is 4.3–45 ns, consistent with $\tau_e \geq 1.2$ ns inferred from the value of p. Interestingly, a suggested semiempirical procedure[55] for calculating exciplex quenching rate constants predicts k_{qe}^{py} values several orders of magnitude smaller than those obtained experimentally. The assumption that in benzene/pyridine mixtures τ_e is independent of solvent polarity cannot be extended to neat pyridine. Extrapolation of the line for eq 14 to [PY] = 12.4 M predicts p_{py} = 0.100 for pyridine solvent. The more than twofold larger experimental value (Table V) no doubt reflects a smaller $k_{-e}\tau_e$ term in p_{py}. This result can be accommodated either by a marked decrease in τ_e and/or by a more modest decrease in k_{-e} upon changing the solvent from benzene or benzene/pyridine mixtures to pyridine.

The efficiency of ^{1}(DCA)* quenching by azulene in benzene was determined in order to interpret its effect on photocycloaddition quantum yields. Since azulene has a window at the wavelengths of DCA excitation and emission, its presence did not interfere with measurement of DCA fluorescence in any trivial way. The results in Table VI-S follow the Stern–Volmer relationship closely ($r^2 = 0.999$, intercept = 1.003) and give $k_{qm}^{az}\tau_m^{ox}$ = 135 M^{-1} at 25 °C. With the lifetime of ^{1}(DCA)* in air-saturated solution (Table IV), $k_{qm}^{az} = 1.79 \times 10^{10}$ M^{-1} s^{-1} is obtained. Since this value is a factor of 2 larger than the rate constant expected for a diffusion-controlled process under these conditions (Table V), it is likely that long-range singlet energy transfer is involved[56] in part.

(55) Caldwell, R. A.; Creed, D.; DeMarco, D. C.; Melton, L. A.; Ohta, H.; Wine, P. H. *J. Am. Chem. Soc.* **1980**, *102*, 2369.

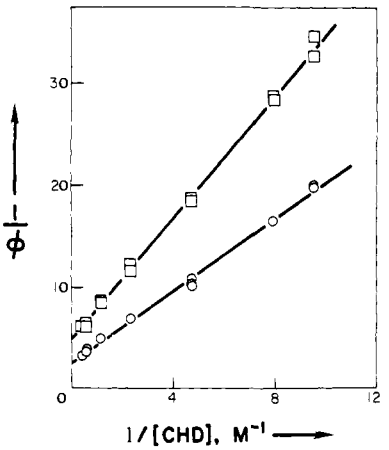

Figure 3. DCA loss (O) and 1,2-adduct quantum yield dependence on [CHD] in degassed benzene (UV).

Photochemical Kinetics. According to Scheme II, ^{1}(DCA·CHD)* is the common precursor for all major DCA-derived products,

$$^1(\text{DCA·CHD})^* \xrightarrow{k_{pe}} \alpha_{14}\text{1,4-Ad} + \alpha_{12}\text{1,2-Ad} + \alpha_{910}\text{9,10-Ad} + \alpha_{24}(?)\text{2,4-Ad} + \alpha_{\text{MCA}}\text{MCA} \quad (15)$$

where $\alpha_p k_{pe}$ is the rate constant for the singlet exciplex pathway leading to product p. A question mark is shown next to α_{24} in eq 15 because the [2 + 4] adduct could not be detected at the low conversions employed for the quantum yield experiments. Since the remaining photoproducts account for ~99% of consumed DCA, the forthcoming discussion requires no assumptions concerning the [2 + 4] adduct. Formation of 9-chloroanthracene, which was detected only in acetonitrile and which did not exceed 5% of the DCA loss except when water was added to the irradiated solutions (Table II), will be discussed separately below. The relationship $(\alpha_{14} + \alpha_{12} + \alpha_{910}) \simeq 1.0$ is nearly exact for most of the experiments described here.

Application of steady-state approximations for all excited species in Scheme II predicts

$$(\phi_{-\text{DCA}})^{-1} = (\phi_{-\text{DCA}}^{\text{lim}})^{-1}\left(1 + \frac{1}{pk_e\tau_m[\text{CHD}]}\right) \quad (16)$$

as the relationship between $\phi_{-\text{DCA}}$ and [CHD] where $\phi_{-\text{DCA}}^{\text{lim}} = k_{pe}\tau_e$ is the limiting quantum yield for DCA loss obtained by extrapolation to infinite [CHD]. Expressions for the dependence of photoproduct quantum yields on [CHD] can be obtained from eq 16 by multiplying $\phi_{-\text{DCA}}^{\text{lim}}$ by the appropriate α_p from eq 15,

$$(\phi_p)^{-1} = (\phi_p^{\text{lim}})^{-1}\left(1 + \frac{1}{pk_e\tau_m[\text{CHD}]}\right) \quad (17)$$

where $\phi_p^{\text{lim}} = \alpha_p\phi_{-\text{DCA}}^{\text{lim}}$. Equations 17 are consistent with the observation that, within experimental uncertainty, adduct quantum yields are independent of [CHD] (see above).

Plots of ϕ^{-1} vs. $[\text{CHD}]^{-1}$ are linear as expected from eq 16 and 17; Figure 3 is typical. Limiting quantum yields obtained from the intercepts and $pk_e\tau_m$ values obtained from intercept/slope, i/s, ratios of these plots are listed in Table VI. Generally, quantum yields obtained by UV analysis are considered more reliable. It can be seen that i/s ratios from these experiments give $pk_e\tau_m$ values in excellent agreement with those obtained from the Stern–Volmer plots (Table V). The poor agreement between $pk_e\tau_m$ from the fluorescence data and the i/s ratios for $\phi_{-\text{DCA}}$ and $(\phi_{1,2} + \phi_{1,4})$ in toluene reflects analyses problems in the earliest GLC experiments and is not considered meaningful. Careful examination of the photoreaction in benzene by UV and ^{1}H NMR spectroscopy (Table I) reveals no change in adduct distribution

(56) Bennett, R. G.; Kellogg, R. E. *Prog. React. Kinet.* **1967**, *4*, 215.

Table VI. Intercept/Slope Ratios and ϕ^{lim} Values from ϕ^{-1} vs. $[CHD]^{-1}$ Plots

	source, i/s =			
solvent	ϕ_{-DCA}	$\phi_{9,10}$	$\phi_{1,2}$	$\phi_{1,2} + \phi_{1,4}$
C_6H_6[a]	1.42 ± 0.06		1.54 ± 0.07	
C_5H_5N[a]	14.5 ± 0.5		12.6 ± 0.6	
CH_3CN[a]	15.6 ± 1		11.4 ± 0.6	
CH_3CN[b]	12.7 ± 3	7.2 ± 2		16 ± 3
CH_3CN[b,c]	8.0 ± 7	4.9 ± 0.5		12 ± 6
$C_6H_5CH_3$[b]	2.2 ± 0.2	0.89 ± 0.1		4.6 ± 0.5
	ϕ_{-DCA}^{lim}	$\phi_{9,10}^{lim}$	$\phi_{1,2}^{lim}$	$\phi_{1,2}^{lim} + \phi_{1,4}^{lim}$
C_6H_6[a]	0.40 ± 0.02		0.21 ± 0.01	
C_5H_5N[a]	0.030 ± 0.01		0.022 ± 0.002	
CH_3CN[a]	0.24 ± 0.02		0.182 ± 0.010	
CH_3CN[b]	0.29 ± 0.06	0.10 ± 0.02		0.19 ± 0.04
CH_3CN[b,c]	0.29 ± 0.15	0.10[d]		0.16 ± 0.10
$C_6H_5CH_3$[b]	0.24 ± 0.02	0.22 ± 0.03		0.08 ± 0.01

[a] UV analyses. [b] GLC analyses. [c] Air-saturated. [d] Assumed.

between 0.05 and 2.20 M diene and thus disproves the apparent dependence noted in the toluene experiments. The GLC experiments in acetonitrile, for which much care was taken to avoid problems encountered with the analysis of toluene samples, are in satisfactory agreement with the corresponding UV results. The limiting product quantum yields in Table VI are in excellent agreement with the product distributions obtained in the preparative experiments (Table I), the only exception being $\phi_{9,10}^{lim}$ in acetonitrile, which is about three times the value expected from the experiment in Table I. It can be seen from Table II that experiments carried out to low DCA conversions give consistently larger 9,10-adduct yields that are independent of [CHD] in degassed or air-saturated acetonitrile solutions. Taken together, the results are consistent with Scheme II in which at least the 9,10-, 1,2-, and 1,4-adduct arise from a common singlet exciplex intermediate in all solvents employed in this work.

Results obtained in air-saturated acetonitrile, though less reproducible than those from degassed solutions, are also consistent with Scheme II, including eq 7 and 8. In the presence of molecular oxygen, the expected relationship between quantum yields and [CHD] is the same as in eq 16 and 17, except that p is replaced by p^{ox} (eq 10) τ_m by $\tau_m^{ox} = (k_{fm} + k_{ism} + k_{qm}[O_2])^{-1}$, and ϕ^{lim} by $\phi^{lim,ox} = \phi^{lim}(1 + k_{pe}^{ox}\tau_e[O_2])^{-1}$. Plots of $(\phi_{-DCA}^{ox})^{-1}$ and $(\phi_p^{ox})^{-1}$ vs. $[CHD]^{-1}$ have i/s ratios in satisfactory agreement with the spectroscopically determined $p_{ox}k_e\tau_m^{ox} = 9.64\ M^{-1}$ value (Table VI). Though the scatter of the ϕ^{ox} values is large, it is noteworthy that intercepts obtained are nearly identical with those for degassed solutions. This result is consistent with the spectroscopic observations since it requires that ^{1}(DCA·CHD)* be too short-lived to be quenched by O_2 in air-saturated acetonitrile, i.e., $k_{qe}^{ox}\tau_e[O_2] << 1$ so that $\phi^{lim} = \phi^{lim,ox}$.

The tenfold decrease in limiting quantum yields for loss of DCA and cycloadduct formation in neat pyridine strongly supports the proposed quenching of the product precursor, ^{1}(DCA·CHD)*, by pyridine. Comparable ϕ^{lim} values for benzene and acetonitrile show that these parameters are not very sensitive to solvent polarity changes. According to Scheme II, including eq 11, the effect of added pyridine on quantum yields in benzene should be given by eq 16 and 17, provided that the change in $pk_e\tau_m$ is taken into account (Table V) and ϕ^{lim} is replaced by $\phi^{lim,py} = \phi^{lim}(1 + k_{qe}^{py}\tau_e[PY])^{-1}$. Using the spectroscopically determined $k_{qe}^{py}\tau_e = 0.31\ M^{-1}$, it can be shown that the expected decreases in the quantum yields at 0.21 M CHD are 21% for [PY] = 0.993 M and 38% for [PY] = 1.99 M. The smaller, somewhat erratic changes obtained experimentally (Table III) are again due to errors introduced by GLC analysis.

If the three major cycloadducts all have a singlet exciplex precursor and there is no triplet pathway to these products, then the minimum effect of azulene on product quantum yields should reflect only azulene's quenching of ^{1}(DCA)*. Larger effects could be accommodated if ^{1}(DCA·CHD)* were also quenched by azulene. The minimum azulene effect on ϕ's can be calculated by replacing τ_m in eq 16 and/or 17 by $\tau_m^{az} = (k_{fm} + k_{ism} + k_{qm}^{az}[AZ])^{-1}$. It follows that this minimum effect is given by

$$(\phi/\phi^{az}) = (\tau_m/\tau_m^{az})(1 + pk_e\tau_m[CHD])/(1 + pk_e\tau_m^{az}[CHD]) \quad (18)$$

where ϕ/ϕ^{az} is the ratio of a specific quantum yield in the absence of azulene to the quantum yield in the presence of azulene. Since k_{qm}^{az}, pk_e, and τ_m have been determined spectroscopically, minimum ϕ/ϕ^{az} ratios can be calculated for any combination of [CHD] and [AZ]; for the experiment in Table III, $(\phi/\phi^{az}) = 1.23$ is predicted. The experimental quantum yields are in excellent agreement with this ratio (Table III): $(\phi_{-DCA}/\phi_{-DCA}^{az}) = 1.20$, $(\phi_{9,10}/\phi_{9,10}^{az}) = 1.27$, $(\phi_{1,2} + \phi_{1,4})/(\phi_{1,2}^{az} + \phi_{1,4}^{az}) = 1.21$, suggesting that at $[AZ] = 1.67 \times 10^{-3}$ M no significant quenching of the exciplex by azulene takes place. This conclusion is somewhat tentative due to the uncertainties in GLC analyses. A larger azulene effect would be expected if ^{3}(DCA)* also gave the cycloadducts since the quenching of ^{3}(DCA)* by azulene is expected to be nearly diffusion controlled.[57]

Adduct Distributions. A simple equation has been proposed recently for predicting reactivity in allowed [2 + 2] and [4 + 4] singlet-state photocycloadditions:

$$\gamma(r_c) = (E_T^A + E_T^B - E_S^A)/c^2 \quad (19)$$

where $\gamma(r_c)$ is the resonance integral for end-on interaction of carbon 2p orbitals at distance r_c, E_T^A and E_T^B are triplet energies of reactants A and B, E_S^A is the singlet energy of the excited reactant A, and c^2 is the sum of HOMO and LUMO orbital coefficient products over reacting positions.[58] The quantity $\gamma(r_c)$ is supposed to be related to the energy of the transition state for cycloaddition; the lower $\gamma(r_c)$, the more favorable the reaction. Since this procedure has met some success in rationalizing the relative reactivity of a variety of addends, it is of interest to determine whether it can predict the adduct distribution in a system such as DCA/CHD where three allowed pathways compete. For the DCA reaction sites, Huckel MO coefficients obtained by using $\alpha_{Cl} = \alpha_0 + 2\beta_0$ and $\beta_{CCl} = 0.4\beta_0$ as coulomb and resonance integrals for Cl,[59] respectively, are within 2–3% of those for anthracene.[60] Together with the diene coefficients they give c^2 values for eq 19 of 1.062, 1.476, and 2.102 for the 1,2-, 1,4-, and 9,10-adduct, respectively. The predicted reactivity order, 9,10- > 1,4- > 1,2-adduct, is clearly at variance with the observed, 1,2- > 9,10- > 1,4-adduct. On the positive side is that substitution of the appropriate energies ($E_T^A = 40.4$,[61] $E_T^B = 53$,[62] $E_S^A = 71.0$ kcal/mol) into eq 19 gives $\gamma(r_c) = 21.1$, 15.2, and 10.7 kmol/mol for the 1,2-, 1,4-, and 9,10-adduct, respectively, all within the limit $\gamma(r_c) \leq 22$ kcal/mol for which other reactions have nearly diffusion-controlled rate constants.[58]

9-Chloroanthracene Formation. When DCA is irradiated in the presence of 2,5-dimethyl-2,4-hexadiene (DMH) in acetonitrile, 9-chloroanthracene (MCA) is the only DCA-derived product.[49] Evidence has been presented that implicates singlet exciplex, triplex and ion–radical intermediates in this reaction, with displacement of chlorine occurring via protonation of relatively long-lived DCA anion radicals ($DCA^{-}\cdot$).[49] The postulated transient formation of $DCA^{-}\cdot$ has since been confirmed spectroscopically.[63] A generalized mechanism for diene-induced photodechlorination of DCA may thus be formulated as

(57) Herkstroeter, W. G. *J. Am. Chem. Soc.* **1975**, *97*, 4161.
(58) Caldwell, R. A. *J. Am. Chem. Soc.* **1980**, *102*, 4004.
(59) Steitwieser, A., Jr. "Molecular Orbital Theory for Organic Chemists"; Wiley: New York, 1961; p 125.
(60) Coulson, C. A.; Streitwieser, A., Jr. "Dictionary of π-Electron Calculations"; Freeman: San Francisco, 1965.
(61) Padye, M. R.; McGlynn, S. P.; Kasha, M. *J. Chem. Phys.* **1956**, *24*, 588.
(62) Kellog, R. E.; Simpson, W. T. *J. Am. Chem. Soc.* **1965**, *87*, 4230. Evans, D. F. *J. Chem. Soc.* **1960**, 1735.
(63) Bonneau, R.; Saltiel, J., unpublished results.

$$^1DCA^* + \text{diene} \rightleftarrows {}^1\text{exciplex}^* \rightarrow DCA^{-}\cdot + \text{diene}^{+}\cdot + \Delta G_{et} \quad (20)$$

$$\text{diene}^{+}\cdot \rightarrow \rightarrow \text{diene and/or diene products} \quad (21)$$

$$DCA^{-}\cdot \xrightarrow{H^+} \rightarrow MCA \quad (22)$$

where the final step in eq 20 represents formation of fully solvated ion radicals. The overall change in free energy for the latter step is given by

$$\Delta G_{et} = \Delta G_{23} + e_0^2/\epsilon a \quad (23)$$

where ΔG_{23} represents the free energy change for formation of ion radicals from $^1DCA^*$ and D within a solvent cage,

$$\Delta G_{23} = E(D/D^+) - E(A^-/A) - \Delta E_{00} - e_0^2/\epsilon a \quad (24)$$

and $e_0^2/\epsilon a$ is a coulombic attraction term that accounts for the free energy gained when $A^{-}\cdot$ and $D^{+}\cdot$ are brought within encounter distance a in a solvent of dielectric ϵ.[64] The other terms in eq 24 are the potentials for one electron oxidation of donor D, $E(D/D^+)$, and reduction of acceptor A, $E(A^-/A)$, and the singlet excitation energy of A, ΔE_{00}.[64] The abilities of DMH and CHD to transfer an electron to DCA when serving as donor partners in the singlet exciplex depend on the magnitude of ΔG_{et} in each case. Gas-phase diene ionization potentials (IP),[11e] can be converted to solution-phase oxidation potentials by using an adapted version of an empirical function[65]

$$E(D/D^+) = 0.89(IP) - 6.04 + 0.30 \quad (25)$$

where $E(D/D^+)$ units are volts vs. the standard calomel electrode (SCE) in acetonitrile. The addition of 0.30 in eq 25 is for the change from the $Ag/AgNO_3$ reference potential employed to SCE.[65,66] This gives 1.24 and 1.65 V for DMH and CHD, respectively. The known reduction potential of DCA in acetonitrile, $E(A^-/A) = -1.01$ V vs. Hg,[67] can be adjusted to $E(A^-/A) = -1.51$ V vs. SCE,[66] and the onset of DCA fluorescence in acetonitrile gives $E_{00} = 3.08$ eV. Substitution of the above parameters into eq 23 and 24 gives $\Delta G_{et} = -7.6$ and $+1.8$ kcal/mol for DMH and CHD, respectively. The estimated minimum uncertainty in these numbers if ±2 kcal/mol. It can be seen that while electron transfer from DMH to $^1DCA^*$ remains exothermic within this uncertainty range, the corresponding process with CHD may be substantially endothermic, thus accounting for the sharp reduction in the efficiency of MCA formation when CHD is substituted for DMH. Furthermore, in the case of DMH, a constant fraction, if not all, of the $DCA^{-}\cdot$ formed is converted to MCA independent of the concentration of added water, suggesting $DMH^{+}\cdot$ is rapidly destroyed and back electron transfer does not complete with protonation of $DCA^{-}\cdot$.[49] In the case of CHD, on the other hand, back electron transfer should be exothermic and probably much more efficient. This is consistent with the increase in ϕ_{MCA} (Table II) from 0.0021 in the absence of added water to 0.0070 and 0.0086 at 0.56 and 1.11 M H_2O, respectively. The involvement of $DCA^{-}\cdot$ in MCA formation when CHD is employed is indicated by the complete suppression of MCA formation when air-saturated acetonitrile solutions are employed (Table II).[49,63]

Experimental Section

Materials. 9,10-Dichloroanthracene (K & K, reagent) was dissolved in CCl_4, passed through a short alumina column, freed of anthracene (~0.04%, GLC) and 9-chloroanthracene (~1.1%) by three recrystallizations from CCl_4/CH_3OH solvent mixtures, and vacuum sublimed twice to give bright yellow crystals (99.9+ % DCA by GLC, ^1H NMR); mp 211.9–212.9 °C. 9-Chloroanthracene (Pfaltz and Bauer, reagent) was passed through a short alumina column with *n*-heptane as eluent, freed of anthracene (~3%, GLC) and DCA (~5%) by using preparative-scale TLC (silica gel, *n*-heptane) or preparative-scale GLC (10% DC-710 silicon oil on Chromosorb W), recrystallized from methanol, and vacuum sublimed to give pale yellow crystals of 9-chloroanthracene (99+ %, GLC, ^1H NMR); mp 104.2–105.8 °C. Benzophenone (Fisher, certified reagent) was recrystallized from *n*-pentane or diethyl ether two–three times and vacuum sublimed; mp 47.6–48.3 °C. *trans*-Stilbene was either Aldrich (zone-refined, ≤0.01% cis isomer, GLC) or Aldrich (reagent, 96%) twice recrystallized from *n*-heptane, chromatographed on alumina with *n*-hexane as eluent and then sublimed (0.031% cis isomer, GLC); mp 123.1–124.9 °C. 1,3-Cyclohexadiene (Aldrich, 96–99% or Chemical Samples, 99%) was passed through a short alumina column and bulb-to-bulb distilled under vacuum immediately prior to use. Acetonitrile (Matheson, Coleman, and Bell, bulk reagent) was purified by Mann's procedure.[68] Final distillation was from calcium hydride; bp 82.0–82.2 °C. Except for a higher level of fluorescent impurities, spectral grade acetonitrile (Eastman) gave identical results with those obtained with the purified solvent. Benzene (Mallinckrodt, reagent) was purified by the Metts exhaustive photochlorination procedure.[69] Benzene-d_6 (Baker, 99.5 atom % D; Stohler Isotope, 99.5 atom % D) was used as received. Toluene (Mallinckrodt, reagent) was purified as previously described.[69b] Pyridine (Mallinckrodt, spectral grade) was distilled on a 1.3 cm o.d. × 100 cm vacuum-jacketed fractionating column packed with stainless steel helices (Helipac, Podbielniac Corp.); bp 115.6–115.8 °C. Azulene (Aldrich, 99%) was chromatographed on alumina with *n*-pentane eluent, recrystallized from *n*-pentane, and vacuum sublimed; mp 98.9–99.9 °C.

Fluorescence Measurements. A Perkin-Elmer Hitachi MPF-2A spectrophotometer equipped with a 150-W Xenon lamp, R-106 photomultiplier, and thermostated sample cell holder was employed in the ratio recording mode. Sample temperature was controlled by passing methanol through the cell holder block by using a Haake constant-temperature circulator equipped with a contact thermoregulator and an external cooling circuit (dry ice/isopropanol). Temperature was monitored with an iron–constantan thermocouple placed in a reference cell kept in one of the cell holder compartments. The thermocouple was calibrated against a National Bureau of Standards thermometer. Solutions were allowed to equilibrate in the cell holder at least 15 min prior to taking fluorescence measurements. Pyrex cells constructed from square 1-cm precision-bore tubing (Ace Glass) were attached to degassing bulbs (13-mm o.d. tubing) fitted with 10/30 joints and grease traps. Solutions, ~3 mL, were degassed by using five–six freeze–pump–thaw cycles to about 10^{-6} torr, after which the ampules were flame-sealed at a constriction. The solutions were transferred to the square cell and emission spectra were recorded from two–four separate faces of each cell (±2% agreement). Quartz 1 cm × 1 cm cells fitted with Teflon stoppers were employed in obtaining emission spectra from air- and oxygen-saturated solutions.

Irradiation Procedures. Preparative-scale irradiations were carried out in cylindrical Pyrex Hanovia reactors (0.2–2.0-L capacity) equipped with water-cooled Pyrex lamp probes, Hanovia medium-pressure Hg lamps, 200- and/or 450-W, and fritted-glass bubblers. Solutions were irradiated while a constant stream of nitrogen or argon bubbled through the reaction mixture. Reaction progress was monitored by GLC and/or UV. Solvent and volatile residues were removed either by rotary evaporation at reduced pressure or by bulb-to-bulb distillation under vacuum. Nonvolatile product mixtures were separated by column chromatography on silica gel/10% $AgNO_3$ and/or alumina. Two procedures were employed for analytical-scale irradiations designed to minimize sample handling and any possibility of thermally converting 1,4-adduct to 1,2-adduct. In procedure 1, Pyrex 3-mm NMR tubes fitted with 10/30 ⅁ joints and grease traps were loaded with 0.5-mL samples of benzene-d_6 solutions containing DCA, CHD, and ~0.003 M tetramethylsilane. Solutions were degassed (four freeze–pump–thaw cycles, 10^{-6} torr) and flame sealed. Ampules were immersed in a thermostated water bath or at room temperature (~22 °C) and irradiated either at 404 nm, filter system 2, or at $\lambda > 320$ nm, uranyl glass filter. Reaction mixtures were analyzed in the sealed ampules by 270-MHz ^1H NMR immediately after irradiation. In procedure 2, Pyrex 13 × 100 mm test tubes equipped with 10/30 ⅁ joints, grease traps, and cylindrical 13 × 100 mm distillation bulbs were loaded with 3.0-mL solutions. Solutions were degassed (five–six cycles, 10^{-6} torr) and the ampules flame-sealed at a constriction. Irradiations were in a merry-go-round apparatus[24] immersed in a thermostated water bath. Excitation was at 404 nm, filter system 2. Solvent and unreacted diene were removed by vacuum bulb-to-bulb distillation

(64) (a) Rehm, D.; Weller, A. *Isr. J. Chem.* **1970**, *8*, 250. (b) Rehm, D.; Weller, A. *Ber. Bunsenges. Phys. Chem.* **1969**, *73*, 834. (c) Knibbe, H.; Rehm, D.; Weller, A. *Ibid.* **1968**, *72*, 257.

(65) Miller, L. L.; Nordblom, G. D.; Mayeda, E. A. *J. Org. Chem.* **1972**, *37*, 916.

(66) Mann, C. K.; Barnes, K. K. "Electrochemical Reactions in Nonaqueous Systems"; Marcel Dekker: New York, 1970; pp 20–27.

(67) Marcondes, M. E. R.; Toscano, V. G.; Weiss, R. G. *J. Am. Chem. Soc.* **1975**, *97*, 4485.

(68) O'Donnel, J. F.; Ayres, J. T.; Mann, C. K. *Anal. Chem.* **1965**, *37*, 1161.

(69) (a) Metts, L.; Saltiel, J., unpublished results. (b) Saltiel, J.; Marchand, G. R.; Smothers, W. K.; Stout, S. A.; Charlton, J. L. *J. Am. Chem. Soc.* **1981**, *103*, 7159.

(~23 °C) into the cylindrical side arm. Crystalline residues were dissolved in benzene-d_6 and analyzed by 270-MHz ^{1}H NMR. In a few cases, duplicate irradiated ampules were broken open immediately following the irradiation and analyzed by UV. The merry-go-round apparatus was also used for quantum yield measurements. A calibrated 5-mL syringe was used to deliver 3.0-mL aliquots to 13 × 100 mm ampules fitted with grease traps and 10/30 ⅋ joints. Solutions were degassed (four–six freeze–pump–thaw cycles, 10^{-6} torr) and the ampules flame sealed at a constriction. In most experiments, extra tubes were degassed and used as reference samples for UV measurements. Ampules containing air-saturated solutions were loosely sealed with 10/30 ⅋ glass stoppers. Benzophenone-sensitized photoisomerization of *trans*-stilbene in degassed benzene ($\phi_{t\to c}$ = 0.55[25,26]) was used for actinometry. Actinometer conversions were corrected for back reaction and zero-time *cis*-stilbene content.[27]

Light Filters and Lamps. Hanovia medium-pressure Hg lamps (200, 450, or 550 W; Ace Glass, Inc.) were employed. Filter system 1, consisting of a combination of Corning CS 7-37 and CS 0-52 glass filter plates that transmits a band of UV light between 355 and 380 nm, was used to isolate the group of mercury lines at 366 nm. Filter system 2 consisted of a uranyl glass sleeve and a 1-cm path length of filter solution, 1 L of which was prepared by dissolving $NaNO_2$ (30 g), $CuSO_4{\cdot}5H_2O$ (27 g), and concentrated NH_4OH (50 mL) in water. This system transmits a band of light between 395 and 490 nm and was employed in the 404-nm excitation experiments. Filter system 3 was used to isolate the 313-nm Hg line. It consisted of a 0.2–0.3-cm path length of a solution prepared by diluting $K_2Cr_2O_7$ (1.0 g) and K_2CO_3 (15.0 g) to 500 mL with water and a set of Corning CS 7-54 glass filter plates.

Absorption Measurements. UV spectra were recorded at room temperature on Cary 14 or Cary 15 spectrophotometers. NMR spectra were obtained on Varian HA-60, Brüker HX-90, or Brüker HX-270 MHz instruments with tetramethylsilane (Aldrich, NMR grade) as internal standard. IR spectra were obtained on a Perkin Elmer Model 257 grating spectrophotometer with KBr pellets.

Gas–Liquid Chromatography. Quantitative GLC analyses were carried out on a Varian-Aerograph Model 2700 gas chromatograph (flame ionization detectors). The recorders, a Sargent Model SR and a Leeds and Northrup Speedomax W, were equipped with disk integrators. Preparative GLC was done with a Varian Aerograph Model 700 instrument equipped with a thermal conductivity detector and a Varian Model G-4010 recorder. Stilbene actinometer solutions were analyzed by using matched $^1/_8$ in. × 5 ft stainless steel columns packed with 7% Apiezon M on Supelcoport (100–120 mesh) operated over a programmed temperature range of 175 → 210 °C (4 °C/min). Solutions were concentrated on a warm hot plate under a gentle stream of N_2 while gradually replacing the original solvent with CCl_4 or CS_2. DCA/CHD reaction mixtures were analyzed on matched $^1/_8$ in. × 1.5 ft stainless steel columns (on column injection) packed with 0.1% Carbowax 20-M on Supelcoport (100–120 mesh). The following describes optimum operation conditions. Injection ports and flame detectors were maintained at 145 and 350 °C, respectively. Columns were operated by using sequential programmed temperature ranges (25 °C/min) of 100 → 140 °C, giving anthracene, MCA, and DCA; 140 → 165 °C, giving 9,10-adduct; and 165 → 190 °C, giving the 1,2-adduct. Control runs with pure adducts established that the [2 + 4] and 9,10-adducts have identical retention times. Comparison of GLC results with 270-MHz ^{1}H NMR and/or UV results for the same mixtures established identical retention times for the 1,2- and 1,4-adducts. The relative molar response of the GLC detector to DCA and 1,2-adduct, 1.00:1.30 ± 0.02 was applied in correcting all adduct areas. Samples from the DCA/CHD system were freed of solvent and unreacted diene by vacuum bulb-to-bulb distillation, 23 °C, leaving crystalline residues, which were dissolved in CCl_4 and GLC analyzed. The above procedure gave DCA losses in excellent agreement with UV measurements (Table II). Initial GLC analyses employed variations of this procedure in which several problems were noted: (a) injection temperatures above 160 °C lead to significant increases in DCA peak areas due to adduct fragmentation (primarily 1,2-adduct; 1,4- → 1,2-adduct Cope rearrangement appears to be complete at lower injection temperatures, 130–155 °C); (b) injection temperatures below 125 °C could not be employed due to condensation of DCA and adducts at the injection port; (c) results depend on the "age" of the GLC columns (previously unused columns give higher relative yields for the 1,2-adduct in better agreement with UV analyses). In addition, prolonged exposure of samples to air, particularly those containing high [CHD] must be avoided because it results in substantial decrease in the relative 1,2- plus 1,4-adduct GLC area. A combination of these problems account for relatively high $\phi_{9,10}$ values in Table III.

1,4- and 1,2-Adduct Stability. The thermal conversion of 1,2-adduct to 1,4-adduct and the photolysis of both adducts (313 nm) or the 1,2-adduct, selectively (366 nm), were studied by UV and/or NMR starting with pure 1,2-adduct, or ~1:1 mixtures of the two adducts. DCA was used as an internal NMR standard in some of the thermal experiments after showing that it is not a product of thermal reaction at $T < 100$ °C. Some experiments were carried out by using degassed ampules provided with square cuvette side arms for UV measurements. DCA/CHD mixtures were irradiated to >98% DCA loss (404 nm) and the adducts cleaved by excitation at 305 nm from a Bausch and Lomb super-high-pressure Hg source grating monochromator. In other cases, solutions containing adducts were irradiated (313 nm) directly in degassed NMR tubes. No photointerconversion of adducts was detected.

Photoadduct Characterization. Adduct samples used for spectroscopic measurements were purified by column chromatography on silica gel/10% $AgNO_3$ with *n*-hexane/10–50% benzene as eluent, followed by repeated recrystallizations from *n*-heptane.

9,10-Dichloro-11,12,13,14-tetrahydro-9,10[1′,4′]-benzenoanthracene (9,10-adduct): white crystals; mp 173.8–174.7 °C; IR (KBr) 3060, 3040, 2960, 2940, 2860, 1458, 840, 764, 740 cm^{-1}; ^{1}H NMR (270 MHz, $CDCl_3$) δ 1.4–1.7 (m, 4 H, methylene), 3.4–3.5 (br s, 2 H, bridgehead), 5.6–5.7 (dd, 2 H, vinyl), 7.3–7.4 (m, 4 H, aromatic), 7.9–8.1 (m, 4 H, aromatic); UV (cyclohexane) λ_{max} 278 nm (ϵ = 610 M^{-1} cm^{-1}), 270 (520), 220 (sh 19 600). Chemical analysis. Calcd for $C_{20}H_{16}Cl_2$: C, 73.40; H, 4.93; Cl, 21.67; Found: C, 73.33; H, 4.96; Cl, 21.62.[70]

9,10-Dichloro-11,12,13,14-tetrahydro-9,10[1′,2′]-benzenoanthracene ([2 + 4] adduct): white crystals, mp 129.6–130.9 °C; IR (KBr) 3060, 3030, 2920, 2850, 1450, 932, 769, 729, 711 cm^{-1}; ^{1}H NMR (270 MHz, $CDCl_3$)

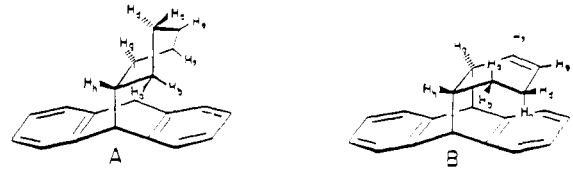

δ 0.8–0.9 (m, 1 H, b), 1.6–1.7 (m, 2 H, cd), 2.0–2.1 (m, 1 H, a), 2.4–2.5 (m, 1 H, h), 2.6–2.7 (d, 1 H, g), 5.7–5.8 (m, 1 H, e), 6.0–6.1 (d, 1 H, f), 7.2–7.3 (m, 4 H), 7.6–7.7 (m, 2 H), 7.7–7.8 (m, 2 H) (The assignments refer to the labeling shown in conformations A and B. Dreiding models indicate that only proton H_b lies directly in the shielding cone of an aromatic ring in A, whereas B places only the allylic protons H_c and H_d in close proximity to this cone.[71] Preference for conformer A and the above assignments are based on the following spin–spin decoupling observations: with decoupling frequency (F_2) on the signal at δ 0.9, the signals at δ 1.7, 2.1, and 2.5 collapse to broad singlets; with F_2 at δ 1.7, the signal at δ 0.9 collapses to a triplet, the signal at δ 2.1 collapses to a pair of doublets, and the multiplet at δ 5.8 collapses to a doublet; with F_2 at δ 2.1, the signal at δ 0.9 simplifies, the multiplet at δ 1.7 becomes a broad singlet, and the multiplet at δ 2.5 collapses to a triplet; with F_2 on the multiplet at δ 2.5, the signals at δ 0.9 and 2.1 simplify and the doublet at δ 2.7 collapses to a singlet; with F_2 on the signal at δ 2.7, the multiplets at δ 2.5 and 5.8 simplify; with F_2 on the signal at δ 5.8, the multiplet at δ 1.7 and the doublet at δ 6.1 collapse to singlets; with F_2 centered on the signal at δ 6.1, the multiplet at δ 5.8 collapses to a singlet); UV (cyclohexane) λ_{max} 270 nm (ϵ = 450 M^{-1} cm^{-1}), 261 (602). Chemical analysis. Calcd for $C_{20}H_{16}Cl_2$: C, 73.40; H, 4.93; Cl, 21.67; Found: C, 73.38; H, 4.97; Cl, 21.60.

1,2,11,12,13,14-Hexahydro-9,10-dichloro-1,2[1′,2′]-benzenoanthracene (1,2-adduct): white crystals, air-sensitive, mp 140–145 °C (decomposition); IR (KBr) 3020, 2820 (br s), 2750, 1264, 769 cm^{-1}; ^{1}H NMR (270

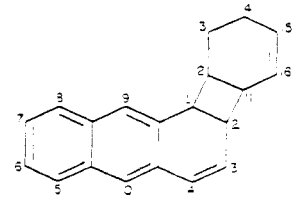

MHz, $CDCl_3$) δ 1.3–1.4 (m, 2 H, H_{13}), 1.7–1.9 (m, 2 H, H_{14}), 3.0–3.2 (quin, 1 H, H_{12}), 3.4–3.5 (br t, 1 H, H_{11}), 3.5–3.7 (m, 1 H, H_2), 4.2–4.3 (t, 1 H, H_1), 5.6–5.8 (br d, 1 H, H_{16}), 5.9–6.0 (m, 1 H, H_{15}), 6.0–6.2 (dd, 1 H, H_3), 7.0–7.1 (dd, 1 H, H_4), 7.4–7.6 (m, 2 H), 8.1–8.3 (m, 2 H, H_5–H_8) (Proton assignments referring to the numbering scheme are supported by the following spin–spin decoupling observations: with F_2 centered on multiplet at δ 8.2, the signal at δ 7.5 collapses to a singlet;

(70) All chemical analyses by Atlantic Microlab, Inc., Atlanta, GA 30366.
(71) Silverstein, R. M.; Bassler, G. C.; Morrill, T. C. "Spectrometric Identification of Organic Compounds", 3rd ed.; Wiley: New York, 1974; pp 159–199.

with F_2 on the signal at δ 7.5, the multiplet at δ 8.2 collapses to a doublet; with F_2 on the signal at δ 7.1, the pair of doublets at δ 6.1 collapse to a doublet; with F_2 centered on the pair of doublets at δ 6.1, the pair of doublets at δ 7.1 collapse to a doublet and the multiplet at δ 3.6 collapses to a triplet; with F_2 centered on the multiplet at δ 5.9, the multiplet at δ 5.7 collapses to a broad singlet; with F_2 centered on the multiplet at δ 5.7, the multiplet at δ 5.9 simplifies and the multiplet at δ 3.4 collapses to a triplet; with F_2 centered on the multiplet at δ 3.4, the multiplet at δ 5.7 simplifies, the multiplet at δ 3.6 collapses to a doublet, and the quintet at δ 3.1 collapses to a quartet); UV (acetonitrile) λ_{max} 362 nm (ϵ = 382 M^{-1} cm^{-1}), 344 (527), 317 (15 300), 304 (17 800), 260 (40 200) (λ (ϵ) used for UV analyses are 317 nm (1.53 × 10^4 M^{-1} cm^{-1}), 319 (1.64 × 10^4), 318 (1.51 × 10^4), 320 (1.59 × 10^4) for acetonitrile, benzene, cyclohexane, and pyridine, respectively). Chemical analysis. Found: C, 73.33; H, 4.97; Cl, 21.63.

1,4,11,12,15,16-Hexahydro-9,10-dichloro-1,4[1′,4′]-benzenoanthracene (1,4-adduct): ^{1}H NMR (270 MHz, $CDCl_3$) δ 1.2–1.5 (m, 4 H, H_{15},

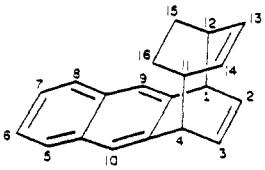

H_{16}), 3.1–3.2 (br s, 2 H, H_{11}, H_{12}), 4.5–4.6 (m, 2 H, H_1, H_4), 6.0–6.1 (dd, 2 H, H_{13}, H_{14}), 6.3–6.4 (dd, 2 H, H_2, H_3), 7.5–7.6 (dd, 2 H, aromatic), 8.2–8.3 (dd, 2 H, aromatic) (Proton assignments referring to the numbering scheme are supported by the following spin–spin decoupling observations: with F_2 centered on the multiplet at δ 8.3, the multiplet at δ 7.6 collapses to a singlet; with F_2 centered on the multiplet at δ 7.6, the multiplet at δ 8.3 collapses to a singlet; with F_2 centered on the multiplet at δ 6.4, the multiplet at δ 4.5 collapses to a doublet); UV (cyclohexane) λ_{max} 326 mm (ϵ = 390 M^{-1} cm^{-1}), 301 (5.07 × 10^3), 292 (6.58 × 10^3).[72]

Note Added in Proof: Professor N. C. Yang has informed us that the 1,2-adduct, though not detected in benzene,[4a] was isolated and characterized in his laboratory when acetonitrile was used as irradiation solvent. For a description of this work see Srinivasachar, K. Ph.D. Dissertation, University of Chicago, 1975.

Registry No. DCA, 605-48-1; CHD, 592-57-4; DCA·CHD (9,10 adduct), 83929-13-9; DCA·CHD ((2 + 4) adduct), 83929-14-0; DCA·CHD (1,2 adduct), 83929-15-1; DCA·CHD (1,4 adduct), 83929-16-2.

Supplementary Material Available: Table I-S, a more detailed version of Table II; Tables II-S and III-S, more detailed versions of Table III; Tables IV-S–VII-S, DCA fluorescence quenching by CHD, AZ, and molecular oxygen (8 pages). Ordering information is given on any current masthead page.

(72) Cf. ref 40, p 335, for comparison with UV spectrum of 2,3-dimethylnaphthalene.

Template Effects. 4.[1] Ion Pairing of Aryloxide Ions with Alkali Cations in 99% Me_2SO: Influence on the Rate of Formation of Benzo-18-crown-6 and of Other Williamson-Type Reactions

Gabriello Illuminati,* Luigi Mandolini,* and Bernardo Masci*

Contribution from the Centro di Studio sui Meccanismi di Reazione del Consiglio Nazionale delle Ricerche, c/o Istituto di Chimica Organica, Università di Roma, 00185 Roma, Italy.
Received April 5, 1982

Abstract: The effect of alkali metal ions on the rate of formation of benzo-18-crown-6 in 99% Me_2SO by cyclization of the conjugate base of *o*-hydroxyphenyl 3,6,9,12-tetraoxa-14-bromotetradecyl ether has been quantitatively accounted for according to a scheme involving separate contributions from free (k_i) and cation-paired (k_{ip}) phenoxide ion. The study has included several additional intra- and intermolecular alkylations of phenoxide ions as reference reactions to provide a set of 25 equilibrium constants for the association of five different phenoxides with the five alkali cations. Both Coulombic interaction and coordination with the neutral oxygen donors are important in determining ion pair stability, but the order in all cases is dominated by Coulombic interaction. This suggests contact interaction in the phenoxide–cation pairs, which is also consistent with evidence from the UV spectra. Whereas the rate of formation of B18C6 is depressed by Li^+ ($k_{ip}/k_i < 0.01$), the effect of the other alkali cations is rate enhancing, the maximum catalytic effect being exhibited by K^+ ($k_{ip}/k_i = 100$). In contrast, in the reference reactions the ion pairs with the alkali cations are either negligibly reactive or much less reactive than the free anions. The association constants of the alkali cations with B18C6 have been determined under the same conditions. A comparative analysis of the extent of interaction of the cations with the reactant, transition state, and reaction product of the crown ether forming reaction shows that the transition state binds cations more strongly than either the reactant or reaction product and reveals that cation interaction with both the negative charge and the neutral donors bear significant contributions to the stability of the ion pair transition state. A rationale for the template effect is presented in terms of proximity effects and chemical effects arising from interaction of the cations with the nucleophilic site of the reactant.

That alkali and alkaline earth cations may greatly facilitate the formation of crown ethers in Williamson-type reactions is a well-recognized phenomenon (template effect), which arises from complexation of the crown's precursor around the metal ion leading to what has been called a "pre-crown" complex.[2] In large ring formation, loss of the conformational entropy due to internal rotations around the single bonds of the bifunctional chain precursor provides a major contribution to the free energy of acti-

(1) For Part 3, see ref 4. A preliminary account of a part of this work has been presented at the Fourth International Symposium on Physical Organic Chemistry, September 4–8, 1978, York, U.K.

(2) As a general reference, see: Reinhoudt, D. N.; de Jong, F. In "Progress in Macrocyclic Chemistry"; Izatt, R. M., Christensen, J. J., Eds.; Wiley: New York, 1979; Vol. 1, p 176.

0002-7863/83/1505-0555$01.50/0